Photonic High-Power 160-GHz Signal Generation by Using Ultrafast Photodiode and a High-Repetition-Rate Femtosecond Optical Pulse Train Generator

Jhih-Min Wun, Hao-Yun Liu, Cheng-Hung Lai, Yi-Shiun Chen, Shang-Da Yang, *Member, IEEE*, Ci-Ling Pan, *Fellow, IEEE*, John E. Bowers, *Fellow, IEEE*, Chen-Bin Huang, *Senior Member, IEEE*, and Jin-Wei Shi, *Senior Member, IEEE*

***Abstract*—We demonstrate photonic high-power MMW generation at subTHz (160 GHz) frequencies by using ultrafast near-ballistic unitraveling carrier photodiodes (NBUTC-PD), which have a miniaturized active area (24 μm^2) and flip-chip bonding package for good heat-sinking. Under optical sinusoidal signal excitation with a ~85% modulation depth, 165-GHz optical-to-electrical 3-dB bandwidth, 18-mA saturation current, +5.11-dBm maximum output power at 160-GHz operating frequency has been demonstrated. In order to further mitigate device-heating, we developed a high-power pulsed optical signal source with increased optical modulation depth: a femtosecond optical short-pulse generator with extremely high repetition rate (160 GHz) and pulsewidth as short as 285 fs. With this novel source, we generated high MMW power (+7.8 dBm) with an effective 120% optical modulation depth at 160 GHz directly from the NBUTC-PD.**

***Index Terms*—Photodiode, ultrafast optics.**

I. Introduction

PHOTONIC millimeter-wave (MMW) generation technique has attracted interest in recent years due to several unique advantages as compared to traditional all-electronic based solution in the MMW regime [1]. As an example, by combining ultrafast photodiodes (PDs) with optical signal generation techniques, a single sweep of generated frequency from near dc to subTHz (hundreds of GHz) becomes possible and is useful for a photonic MMW network analyzer (NA) [2]. Compared with traditional MMW NA, this approach eliminates the necessity of different metallic waveguide based NA extenders (for measurements at different MMW bands) over such wide frequency regime (dc to hundreds of GHz). The other important application of MMW photonic techniques is in wireless communication systems [3]–[6]. Extremely high data rate (>25 Gbit/s) for line-of-sight free space data transmission has been demonstrated [3]–[6]. Nevertheless, the output power level of proposed photonic approach is usually not as strong as that of other THz and MMW signal generation schemes [7].

The limited output power of photonic approach seriously constrains the dynamic range [2] and maximum allowable wireless linking distance [3]–[6] of measurement instrument and wireless communication system, respectively. Improving the optical-to-electrical (O-E) bandwidth (~300 GHz) and saturation power (~mW level) of the PD is an important issue to further improve the performance of these systems. The key to achieve high speed with high saturation current (power) of a PD is to downscale its area as well as its depletion layer thickness. A thinner depletion layer has a larger junction capacitance, a shorter carrier transit time, and a higher saturation current [8], [9] so reducing the device active area is thus necessary to sustain a low junction capacitance and achieve very high speed performance. In order to overcome the trade-off between the RC-limited bandwidth and carrier drift-time, the (modified) uni-traveling carrier PD (UTC-PD) [8], [10], [11], triple transit region PD [12], and near-ballistic UTC-PD (NBUTC-PD) [3], [5], [13]–[15], where only electrons with high drift-velocity are active carriers, have been demonstrated. By use of these devices, excellent saturation power performance has been realized.

The other major limiting factor of maximum power from these miniaturized sub-THz PDs is serious device heating and thermal failure [14], [15]. Through the use of flip-chip bonding to improve heat sinking of the PD during high-power operation, enhancement of its saturation current and microwave power has been reported [13]–[16]. Another elegant approach to overcome such a problem is to increase the effective optical modulation depth during fiber delivery through optical signal processing techniques [17]–[20]. Recently, a higher effective modulation depth as compared to using conventional optical

Manuscript received January 29, 2014; revised May 31, 2014; accepted June 4, 2014. This work was supported by Agilent and Asian Office of Aerospace Research and Development (AOARD) under Agilent Technologies Research Grant #3230, AOARD-13-4086, and AOARD-13-4088; and by National Science Council in Taiwan under Grants NSC 100-2112-M-007-007-MY3 and NSC 101-2221-E-007-103-MY3.

J.-M. Wun, C.-H. Lai, and J.-W. Shi are with the Department of Electrical Engineering, National Central University, Taoyuan 320, Taiwan (e-mail: p3984011@hotmail.com; jungle_171@hotmail.com; jwshi@ee.ncu.edu.tw).

H.-Y. Liu, Y.-S. Chen, S.-D. Yang, and C.-B. Huang are with the Institute of Photonics Technologies, National Tsing-Hua University, Hsinchu 300, Taiwan (e-mail: haoyunliu1118@gmail.com; patrick.chenson@gmail.com; sdyang@ee.nthu.edu.tw; robin@ee.nthu.edu.tw).

C.-L. Pan is with the Department of Physics, National Tsing-Hua University, Hsinchu 300, Taiwan (e-mail: clpan@phys.nthu.edu.tw).

J. E. Bowers is with the Department of Electrical and Computer Engineering, University of California, Santa Barbara, CA 93106 USA (e-mail: bowers@ece.ucsb.edu).

Color versions of one or more of the figures in this paper are available online at http://ieeexplore.ieee.org.

Digital Object Identifier 10.1109/JSTQE.2014.2329940

1077-260X © 2014 IEEE. Personal use is permitted, but republication/redistribution requires IEEE permission.
See http://www.ieee.org/publications_standards/publications/rights/index.html for more information.

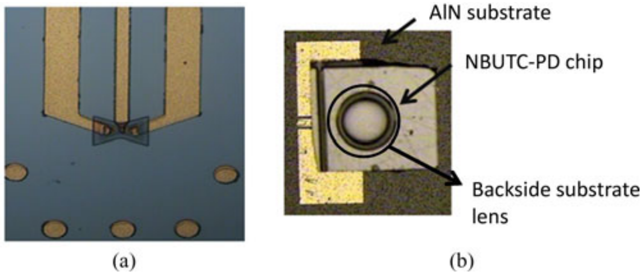

Fig. 1. Top-view of the NBUTC-PD chip before (a) and after flip-chip bonding (b).

sinusoidal excitation has been achieved using a short (<1 ps) optical pulse train with >100 GHz repetition rate [20]. Furthermore, with the decrease in duty cycle of optical short pulse train, a significant improvement (6.4 dB) in saturation MMW power of the ultrafast PD has also been achieved [21]. However, it becomes more difficult to further reduce the pulse-width to the femtosecond regime when the repetition rate of the pulse train reaches hundreds of GHz. This is because the peak optical power of each pulse decreases with the increase of the repetition rate of the pulse train, which would impede the use of nonlinear pulse compression process.

In this paper, we combine the advanced flip-chip bonding process of NBUTC-PD and a novel approach for femtosecond (fs) optical short pulse train generation at a repetition rate of 160 GHz, and the probability of thermal failure of the PD chip under high-power operation has been greatly minimized, which leads to a higher maximum output power. Very-high output power (+7.8 dBm) at 160 GHz operating frequency and a high effective modulation depth (120%) have both been successfully demonstrated.

II. Design of Device Structure and Fabrication

Fig. 1(a) and (b) show the top-view of the NBUTC-PD chip before and after flip-chip bonding, respectively. The detailed epi-layer structure of the PD is shown in Table I and is close to that given in our previous work [15]. Here, we slightly reduce the p-type sheet charge density in the collector layer in order to reduce the optimum bias voltage and device heating under high-power operation. The thickness of the p-type linear graded doped $In_{0.53}Ga_{0.47}As$ based photo-absorption layer (P) is 160 nm. A 120 nm-thick InP layer is utilized as the collector layer (C). The total thickness of the depleted layer under a bias of -2 V is around 200 nm. Based on such epi-layer structure and our bandwidth simulation results, the optimized device active diameter for the maximized 3-dB O-E bandwidth is around 4 μm. It means that with such device size, the simulated *RC*-limited and internal carrier transient time limited bandwidths are nearly balanced. However, in order to have a reasonable high responsivity for practical application of photonic high-power MMW generation, the active diameters of our NBUTC-PDs have been chosen as 5.5 and 6.5 μm (24 and 32 μm^2 active area), which are slightly larger than the optimized size (4 μm in diameter). The measured dc responsivity is around 0.15 A/W. Such value is about twice as large as those of reported near 200 GHz O-E bandwidth UTC-PDs [22] and NBUTC-PDs [15], which usually exhibit responsivity less than 0.08 A/W.

TABLE I
EPI-Layer Structure of NBUCT-PD

Layer	Material	Thickness (Å)	Dopant Level (cm^{-3})/Type	
Graded P-Contact Layer	$In_{0.53}Ga_{0.47}$ As(B)- $In_{0.8}$ $Ga_{0.2}$ As(T)	100	5.0×10^{19}	P+
P-Contact Layer	$In_{0.53}$ $Ga_{0.47}$ As	200	1.0×10^{19}	P+
Diffusion Block	$In_{0.52}Al_{0.29}$ $Ga_{0.19}$ As	200	2.0×10^{18}	P+
Absorption Layer	$In_{0.53}$ $Ga_{0.47}$ As	1,600	$5.0 \times 10^{17}(B) - 5.0 \times 10^{19}(T)$	P+
Graded Layer	$In_{0.52}Al_{0.25}$ $Ga_{0.23}$ As(B)- $In_{0.52}$ $Al_{0.04}$ $Ga_{0.44}$ As(T)	300	2.0×10^{16}	N
Collector Layer	InP	1,200	2.0×10^{16}	N
Charge Layer I	InP	100	1.4×10^{18}	P+
Charge Layer II	InP	50	2.6×10^{16}	PCharge
Layer III	InP	50	6.0×10^{18}	N+
N-Contact Layer	InP	7,000	1.0×10^{19}	N+
N-diffusion block layer	$In_{0.52}Al_{0.48}$ As	2,000		i
Substrate	S.I.Inp			

B: Bottom, T: Top.

Compared with our previous design [15], the geometric size and layout of the flip-chip bonding co-planar waveguide (CPW) pads has further been optimized to not only minimize any ripples on the measured O-E frequency responses from near dc to ~300 GHz, but also to enhance the reliability of our flip-chip bonding process due to the increase in bonding area. The flip-chip bonding substrate is AlN, which has a high thermal conductivity and low dielectric loss. As shown in Fig. 1(a), the three metal stripes on it serve as the CPWs and the marked circle shown on Fig. 1(b) represents the substrate lens on the backside of chip, which improves the alignment tolerance and the responsivity of the PD [14].

III. Measurement Results

The dynamic performance of the PD is measured with a heterodyne beating system. A power meter with two different sensor heads (one for dc to 50 GHz and the other is 75 to 110 GHz) is used for the measurement range from dc to 110 GHz. Above 110 GHz, a thermal MMW power meter (PM4, VDI-Erickson) is used. The maximum measurement bandwidth for our system is limited by our WR-6 waveguide based MMW probe at around 170 GHz. Figs. 2 and 3 show the measured bias-dependent O-E frequency responses of PDs with small (5.5 μm active diameter; device A) and large (6.5 μm active diameter; device B) active area from near dc to 175 GHz under a fixed photocurrent (5 mA). As can be seen, for the case of device A, the bias-dependent speed performance is not significantly changed when the reverse bias voltage increases from -1 V to -3 V. The maximum measured 3-dB O-E bandwidth of device A is

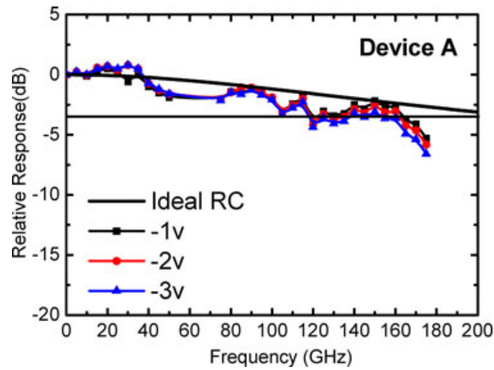

Fig. 2. Measured O-E (close symbols) and extracted *RC*-limited (solid line) frequency responses of device A under different reverse bias (-1 to -3 V) with a fixed 5 mA output photocurrent.

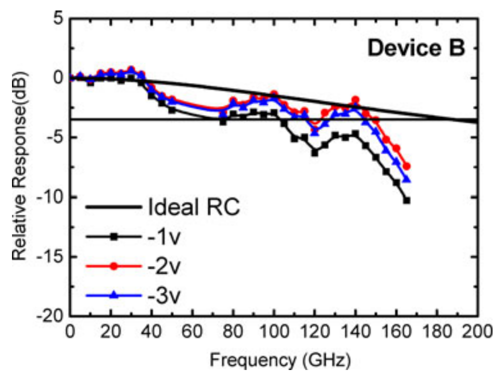

Fig. 3. Measured O-E (close symbols) and extracted *RC*-limited (solid line) frequency responses of device B under different reverse bias (-1 to -3 V) with a fixed 5 mA output photocurrent.

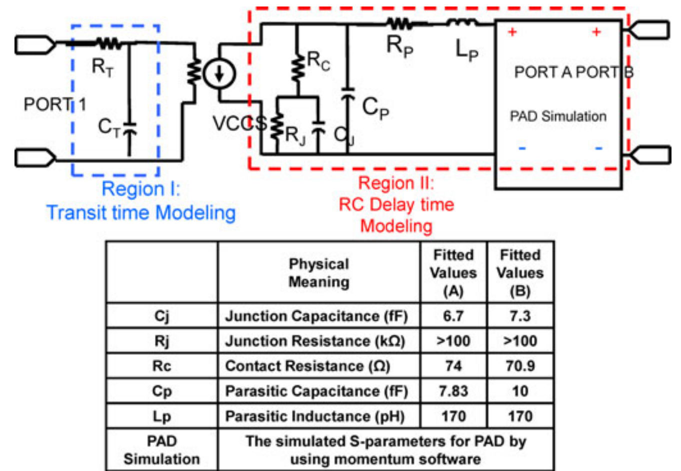

	Physical Meaning	Fitted Values (A)	Fitted Values (B)
Cj	Junction Capacitance (fF)	6.7	7.3
Rj	Junction Resistance (kΩ)	>100	>100
Rc	Contact Resistance (Ω)	74	70.9
Cp	Parasitic Capacitance (fF)	7.83	10
Lp	Parasitic Inductance (pH)	170	170
PAD Simulation	The simulated S-parameters for PAD by using momentum software		

Fig. 4. Equivalent-circuit-model used. The inserted table shows the extracted values of the components. VCCS: voltage controlled current source.

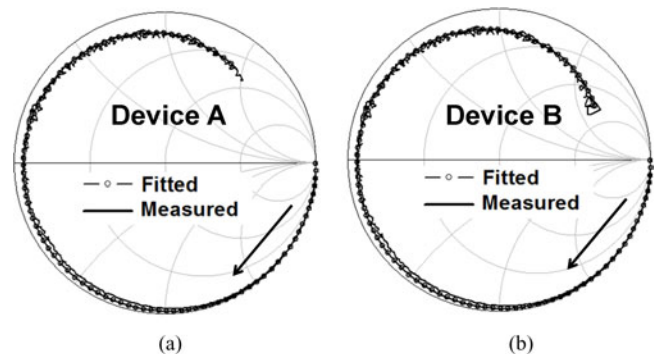

Fig. 5. Measured (continuous line) and fitted (open symbols) S_{11} parameters from near DC to 110 GHz of device A (a) and B (b) under a fixed dc bias (-2 V). The arrow heads indicate the increase in the sweeping frequency.

165 GHz. On the other hand, for the case of device B, there is an increase in the 3-dB O-E bandwidth when the reverse bias voltage increases from -1 to -3 V. Its optimum bias for maximum 3-dB bandwidth performance ($\sim$150 GHz) is at -2 V. The obviously different bias dependence of devices A and B is consistent from device to device on the same wafer. It can be attributed to the influence of device heating (junction temperature) on the dynamic performance. The junction temperature (J_T) of PD is related to the input electrical power (photocurrent $\times$ reverse bias voltage) over its active area [23]. According to the reported values of J_T in high-power UTC-PD [23], the estimated junction temperature of our devices A and B (-3 V bias and 5 mA photocurrent) is over 500 K. Such high value of J_T may diminish the phenomenon of overshoot drift-velocity of electron in the InP based collector layer [24], which plays an important role in the speed performance of UTC-PD with a thin collector layer ($\sim$200 nm) [25]. Due to its smaller active area, we can expect that device A should suffer from more serious device heating and more unobvious phenomenon of electron velocity overshoot as compared to device B. As a result, the electron drift-velocity in the collector layer of device A and its net O-E bandwidth are both less sensitive to the reverse bias voltage.

In order to estimate the 3-dB O-E bandwidth and investigate whether it is the carrier transit time or *RC* (resistance–capacitance) -bandwidth limitation that dominates this device, we adopt two-port equivalent-circuit models, which include the two bandwidth-limiting factors (i.e., carrier transit time (f_t) and *RC* delay time ($f_{\rm RC}$),) [15], as shown in Fig. 4. The values used in fitting process are shown in the Table inserted into Fig. 4. Fig. 5 shows the measured and simulated frequency responses for the S_{11} reflection coefficient parameter under a -2 V bias of device A and B; see the Smith chart. Clearly, the simulated and measured results match very well, from 10 MHz to 110 GHz. Based on the established equivalent circuit model, we can thus extract the *RC*-limited frequency responses of both devices, which are shown as solid line traces in Figs. 2 and 3. As can be seen, the extracted *RC*-limited 3-dB bandwidths of device A and B is 220 and 184 GHz, respectively, and the corresponding f_t is 249 and 260 GHz under -2 V bias. We can thus conclude that the extracted f_t of each structure is close with its $f_{\rm RC}$ and both bandwidth limiting factors have significant influences on the measured net O-E bandwidths. In addition, the slightly larger f_t of device B can be attributed to that it suffers from less device-heating effect than device A does. These conclusions are

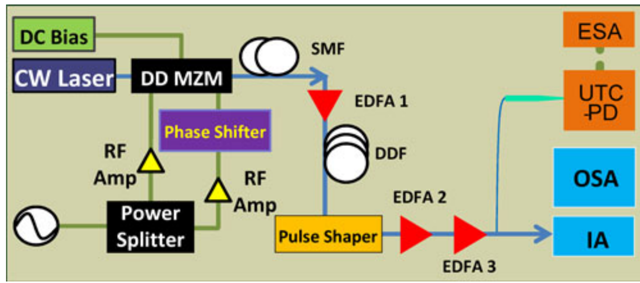

Fig. 6. Schematic of fs optical pulse generator. DD-MZM: dual-drive intensity modulator; EDFA: erbium-doped fiber amplifier; IA: intensity autocorrelator.

supported by our bias dependent speed measurement results, which have been discussed in Figs. 2 and 3.

As discussed in Fig. 2, the device-heating effect has significant influence on the dynamic performance of our devices. To minimize thermal effects and further improve its output power performance, we have designed and constructed a femtosecond optical short pulse generator with extremely high repetition rate at 160 GHz [21]. Fig. 6 shows the schematic of our experimental setup. An externally-modulated continuous-wave laser frequency comb is generated by injecting a narrow-linewidth CW laser into a dual-drive low-V_π $LiNbO_3$ intensity modulator [26]. A 20 GHz sinusoidal signal from an ultra-low phase noise RF signal generator, amplified to +33 dBm, is used to drive the intensity modulator. The modulation frequency of 20 GHz equals the resulting frequency comb line spacing. The details of our home-made line-by-line shaper are described in Ref. [27].

The frequency comb is sent over a spool of single-mode fiber to compensate the quadratic spectral phase [27] so that 3.6 ps transform-limited pulses are generated. The transform-limited pulses are compressed down to 150 fs via adiabatic soliton compression in a dispersion-decreasing fiber (DDF). A flat portion of the resulting spectrally broadened output is used by the line-by-line pulse shaper for pulse train repetition-rate multiplication.

The optical time-domain waveforms are measured using a home-made intensity auto-correlator. The optical spectra are measured using an optical spectrum analyzer with 0.02 nm resolution. In our shaping control, amplitude shaping is applied to remove every other line so the comb spacing is now 40 GHz. The 160 GHz pulse train is then obtained by applying periodic $\{0, 0, \pi, 0\}$ spectral phase filtering onto the remaining 40 GHz comb lines. Such loss-less phase control technique is commonly referred to as temporal Talbot effect [28]. The resulting comb spectrum is shown in Fig. 7(a). Fig. 7(b) shows the experimental intensity autocorrelation traces for the 160 GHz repetition-rate pulse train after applying temporal phase filtering. The solid trace denotes the experimental intensity autocorrelation trace. The dashed trace is the calculated trace obtained by impressing the pulse shaper phase control onto the experimental optical spectrum as shown in Fig. 7(a). The two traces are in excellent agreements. Such intense pulse has a full-width half maximum pulse duration of 285 fs with a low duty-cycle. It is used to enhance the generated MMW signal power as compared to using 160 GHz sinusoidal waveform generated by beating two

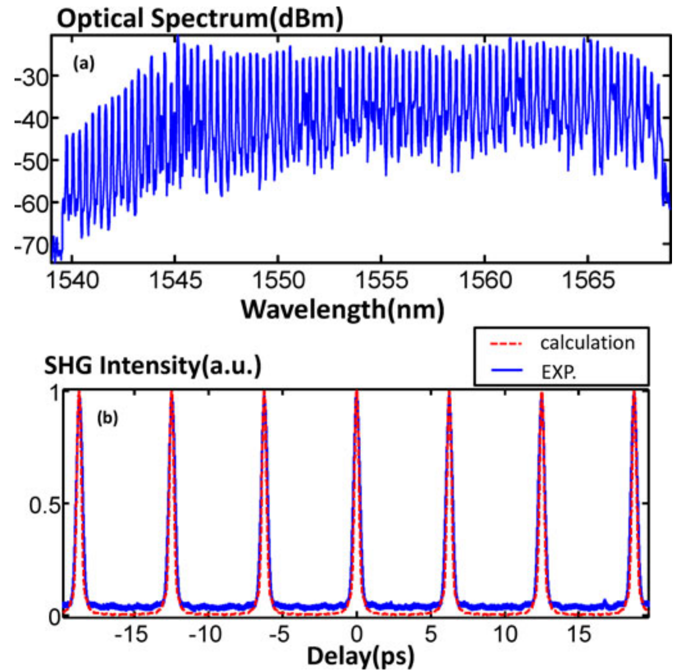

Fig. 7. (a) Line-by-line shaped comb spectrum. (b) The measured and calculated time-domain intensity autocorrelation traces of the 160 GHz pulse train.

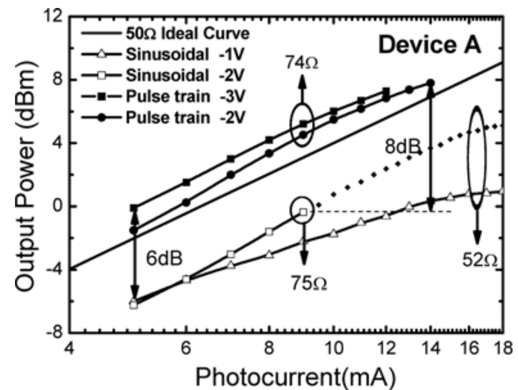

Fig. 8. The Photo-generated MMW power of device A versus output photocurrent under 160 GHz short pulse (close symbols) and 160 GHz sinusoidal signal (open symbols) excitations.

continuous-wave lasers for excitation of the PD. As compared to our previous work [20], the pulse-width is shortened from 2.6 ps to 285 fs due to pulse temporal compressing using the DDF. This much narrower pulse duration allows us in achieving a better pulse repetition-rate multiplication while maintaining a low duty cycle, which is favorable in efficient MMW power generation using short pulses. In our previous theoretical derivation [20], which has assumed that a large enough reverse bias voltage applied onto PDs to minimize the charge screening and field collapse effects under high-power operation, a maximum 6 dB enhancement could be achieved using short optical pulses with low duty cycle as compared to optical sinusoidal waveforms. This is beneficial in mitigating thermal heating in the PD.

Figs. 8 and 9 shows the photo-generated MMW power versus output photocurrent of device A and B under 160 GHz short

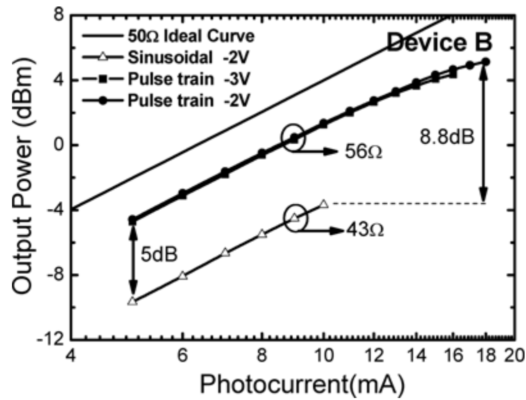

Fig. 9. The photo-generated MMW power of device B versus output photocurrent under 160 GHz short pulse (close symbols) and 160 GHz sinusoidal signal (open symbols) excitations.

pulse (close symbols) or sinusoidal (open symbols) signal excitations (~85% modulation depth), respectively. An ideal line for photo-generated MMW power with a 100% optical modulation depth at a 50 Ω load is also plotted for reference. Irradiated with high optical power, a smaller differential resistance of device would result in less device-heating and a higher saturation power.

In order to let our comparison between sinusoidal and short pulse excitations be fair, we chose the devices under measurement with approximately the same differential resistance for comparison. Their resistance values at a forward-bias current of 5 mA are specified on these two figures. The MMW power shown in here has been de-embedded, taking into account around 3.4 dB loss from the MMW (D-band; 110–170 GHz) probe and waveguide taper (WR-10 to WR-6). Such value of loss was verified independent measurements with the 110–170 GHz network analyzer.

First of all, we can clearly see that under low output photocurrent (5 mA; linear operation) in Figs. 8 and 9, the pulse operation exhibits a 6 and 5 dB enhancement in output power, respectively, as compared to sinusoidal operation. Such number is close to the theoretical prediction (~6 dB) [20]. As shown in Fig. 9, for the case of device B under sinusoidal wave excitation, it usually suffers from thermal failure at 10 mA operation before reaching its maximum saturation output. On the other hand, by use of our pulsed source for device excitation, we can successfully reach the saturation output current of a different device B (with similar value of differential resistance) at 18 mA with a +5.14 dBm output power under −2 V bias. This result clearly indicates that our pulse source can effectively minimize the chance of device thermal failure under high-power operation. Fig. 8 shows the measurement result of device A, which has a wider 3-dB O-E bandwidth (165 vs. 150 GHz) and less high-frequency roll-off than those of device B (−2.6 vs. −6 dB) at 160 GHz. As can be seen, under sinusoidal wave excitation, device A usually suffered from thermal failure at 9~10 mA operation under −2 V bias. Only a few devices on the same chip, which have a lower differential resistance than that of the typical ones (~52 vs. ~75 Ω), can attain a 18 mA saturation current and +5.11 dBm maximum output power (shown as dotted line) under −2 V bias. The sinusoidal measurement result under −1 V bias is shown here for reference. We can clearly see that under low output photocurrent (5 mA), the output MMW power at 160 GHz does not increase at higher values of the reverse bias (−1 to −2 V). Such result is consistent with the measured O-E frequency response, as discussed in Fig. 2. Nevertheless, when the output current increases, a higher reverse bias (−2 V) is still required to compensate space charge screening effect [8] and boost up the generated MMW power.

By using the 160 GHz pulse train, the problem of thermal failure for typical devices can also be mitigated, the same as the case of device B. Therefore, the operation photocurrent can be boosted up to 14 mA. Furthermore, the photo-generated power is even 1.44 times higher than that of the 50 Ω ideal line with a 100% modulation depth under the same operation current. The corresponding effective optical modulation depth is around 120% and the maximum output power is +7.8 dBm under 14 mA operations current. In addition, we can clearly see that by increasing the reverse bias voltage of device A up to −3 V, a slight enhancement in output power can be observed. However, the thermal failure limits its operation current at 12 mA. As specified on this Figure, compared with device A with about the same value of differential resistance (~75 Ω), our short-pulse optical source can offer an enhancement in maximum output power of around 8.2 dB.

This significant enhancement in maximum output power of both devices A and B clearly indicates that pulse-mode operation can really mitigate the thermal failure and device-heating problem, which is really an issue for the miniaturized PD with a sub-THz bandwidth under high-power operation. By combing our optical short pulse train source for photo-generated MMW power enhancement with fast bias modulation characteristic of NBUTC-PD [5], [29], a photonic sub-THz wireless linking with extremely high data rate (>25 Gbit/s) and reasonable wireless linking distance (several meters) can be expected.

IV. Conclusion

In conclusion, by combining the use of a high-power flip-chip bonded NBUTC-PD chip and a photonic sub-THz light source with a pulse-width of 285 fs, we have demonstrated photonic generation of a high-power 160 GHz signal. Compared with the sinusoidal signal, the generated optical pulse train can offer a larger effective modulation depth (120 vs. 85%), save the required optical power, minimize the device-heating problem, and achieve a significant improvement in device maximum output power. By use of such a setup, we can achieve maximum output power as high as +7.8 dBm with a 14 mA photocurrent at 160 GHz operating frequency.

References

[1] A. J. Seeds and K. J. Williams, "Microwave photonics," *J. Lightw. Technol.*, vol. 24, no. 12, pp. 4628–4641, Dec. 2006.

[2] T. Nagatsuma, M. Shinagawa, N. Sahri, A. Sasaki, Y. Royter, and A. Hirata, "1.55-μm photonic systems for microwave and millimeter-wave measurement," *IEEE Trans. Microw. Theory Tech.*, vol. 49, no. 10, pp. 1831–1839, Oct. 2001.

[3] J.-W. Shi, C.-B. Huang, and C.-L. Pan, “Millimeter-wave photonic wireless links for very-high data rate communication,” *NPG Asia Mater.*, vol. 3, no. 2, pp. 41–48, Apr. 2011.

[4] S. Koenig, D. Lopez-Diaz, J. Antes, F. Boes, R. Hennberger, A. Leuther, A. Tessmann, R. Schmogrow, D. Hillerkuss, R. Palmer, T. Zwick, C. Koss, W. Freude, O. Ambacher, J. Leuthold, and I. Kallfass, “Wireless sub-THz communication system with high data rate,” *Nature Photon.*, vol. 7, pp. 977–981, Dec. 2013.

[5] N.-W. Chen, J.-W. Shi, F.-M. Kuo, J. Hesler, T. W. Crowe, and J. E. Bowers, “25 Gbits/s error-free wireless link between ultra-fast W-band photonic transmitter-mixer and envelop detector,” *Opt. Exp.*, vol. 20, no. 19, pp. 21223–21234, Sep. 2012.

[6] H.-J. Song and T. Nagatsuma, “Present and future terahertz communications,” *IEEE Trans. Terahertz Sci. Tech.*, vol. 1, no. 1, pp. 256–263, Sep. 2011.

[7] G. Chattopadhyay, “Technology, capabilities, and performance of low power terahertz sources,” *IEEE Trans. Terahertz Sci. Tech.*, vol. 1, no. 1, pp. 33–53, Sep. 2011.

[8] K. Kato, “Ultrawide-band/high-frequency photodetectors,” *IEEE Trans. Microw. Theory Tech.*, vol. 47, no. 7, pp. 1265–1281, Jul. 1999.

[9] J.-W. Shi, H.-C. Hsu, F.-H. Huang, W.-S. Liu, J.-I. Chyi, J.-Y. Lu, C.-K. Sun, and C.-L. Pan, “Separated-transport-recombination p-i-n photodiode for high-speed and high-power performance,” *IEEE Photon. Technol. Lett.*, vol. 17, no. 8, pp. 1722–1724, Aug. 2005.

[10] H. Ito, S. Kodama, Y. Muramoto, T. Furuta, T. Nagatsuma, T. Ishibashi, “High-speed and high-output InP-InGaAs unitraveling-carrier photodiodes,” *IEEE J. Sel. Topics Quantum Electron.*, vol. 10, no. 4, pp. 709–727, Jul./Aug. 2004.

[11] A. Beling, H. Pan, H. Chen, and J. C. Campbell, “Measurement and modeling of a high-linearity modified Uni-traveling carrier photodiode,” *IEEE Photon. Technol. Lett.*, vol. 20, no. 14, pp. 1219–1221, Jul. 2008.

[12] V. Rymanov, A. Stohr, S. Dulme, and T. Tekin, “Triple transit region photodiodes (TTR-PDs) providing high millimeter wave output power,” *Opt. Exp.*, vol. 22, no. 7, pp. 7550–7558, Apr. 2014.

[13] F.-M. Kuo, M.-Z. Chou, and J.-W. Shi, “Linear-cascade near-ballistic uni-traveling-carrier photodiodes with an extremely high saturation-current-bandwidth product,” *J. Lightw. Technol.*, vol. 29, no. 4, pp. 432–438, Feb. 2011.

[14] J.-W. Shi, F.-M. Kuo, C.-J. Wu, C. L. Chang, C. Y. Liu, C.-Y. Chen, and J.-I. Chyi, “Extremely high saturation current-bandwidth product performance of a near-ballistic uni-traveling-carrier photodiode with a flip-chip bonding structure,” *IEEE J. Quantum Electron.*, vol. 46, no. 1, pp. 80–86, Jan. 2010.

[15] J.-W. Shi, F.-M. Kuo, and J. E. Bowers, “Design and analysis of ultra-high speed near-ballistic uni-traveling-carrier photodiodes under a 50 Ω Load for high-power performance,” *IEEE Photon. Technol. Lett.*, vol. 24, no. 7, pp. 533–535, Apr. 2012.

[16] A. S. Cross, Q. Zhou, A. Beling, Y. Fu, and J. C. Campbell, “High-power flip-chip mounted photodiode array,” *Opt. Exp.*, vol. 21, no. 8, pp. 9967–9973, Apr. 2013.

[17] D. A. Tulchinsky, J. B. Boos, D. Park, P. G. Goetz, W. S. Rabinovich, and K. J. Williams, “High-current photodetectors as efficient, linear, and high-power RF output stages,” *J. Lightw. Technol.*, vol. 26, no. 4, pp. 408–416, Feb. 2008.

[18] U. Gliese, K. Colladay, A. S. Hastings, D. A. Tulchinsky, V. J. Urick, and K. J. Williams, “53.5% photodiode RF power conversion efficiency,” presented at the Opt. Fiber Commun., San Diego, CA, USA, Mar. 2010, Paper PDPA7.

[19] A. Hirata, M. Harada, and T. Nagatsuma, “120-GHz wireless link using photonic techniques for generation, modulation, and emission of millimeter-wave signals,” *J. Lightw. Technol.*, vol. 21, no. 10, pp. 2145–2153, Oct. 2003.

[20] F.-M. Kuo, J.-W. Shi, H.-C. Chiang, H.-P. Chuang, H.-K. Chiou, C.-L. Pan, N.-W. Chen, H.-J. Tsai, and C.-B. Huang, “Spectral power enhancement in a 100-GHz photonic millimeter-wave generator enabled by spectral line-by-line pulse shaping,” *IEEE Photon. J.*, vol. 2, no. 5, pp. 719–727, Oct. 2010.

[21] J.-M. Wun, Y.-S. Chen, C.-H. Lai, H.-Y. Liu, C.-B. Huang, C.-L. Pan, and J.-W. Shi, “Strong enhancement in saturation power of sub-THz photodiode by using photonic millimeter-wave femtosecond pulse generator,” presented at the Opt. Fiber Commun., San Francisco, CA, USA, Mar. 2014, Paper Tu2A.5.

[22] H. Ito, T. Furuta, F. Nakajima, K. Yoshino, and T. Ishibashi, “Photonic generation of continuous THz wave using uni-traveling-carrier photodiode,” *J. Lightw. Technol.*, vol. 23, no. 12, pp. 4016–4021, Dec. 2005.

[23] H. Chen A. Beling, H. Pan, and J. C. Campbell, “A method to estimate the junction temperature of photodetectors operating at high photocurrent,” *IEEE J. Quantum Electron.*, vol. 45, no. 12, pp. 1537–1541, Dec. 2009.

[24] W. Fawcett and G. Hill, “Temperature dependence of the velocity/field characteristics of electron in InP,” *Electron. Lett.*, vol. 11, pp. 80–81, 1975.

[25] T. Ishibashi, “Nonequilibrium electron transport in HBTs,” *IEEE Trans. Electron Devices*, vol. 48, no. 11, pp. 2595–2604, Nov. 2001.

[26] T. Sakamoto, T. Kawanishi, and M. Izutsu, “Asymptotic formalism for ultraflat optical frequency comb generation using a Mach-Zehnder modulator,” *Opt. Lett.*, vol. 32, pp. 1515–1517, 2007.

[27] H.-P. Chuang and C.-B. Huang, “Generation and delivery of 1-ps optical pulses with ultrahigh repetition-rates over 25-km single mode fiber by a spectral line-by-line pulse shaper,” *Opt. Exp.*, vol. 18, pp. 24003–24011, 2010.

[28] C.-B. Huang and Y. C. Lai, “Loss-less pulse intensity repetition-rate multiplication using optical all-pass filtering,” *IEEE Photon. Technol. Lett.*, vol. 12, no. 2, pp. 167–169, Feb. 2000.

[29] F.-M. Kuo, C.-B. Huang, J.-W. Shi, N.-W. Chen, H.-P. Chuang, J. E. Bowers, and C.-L. Pan, “Remotely up-converted 20 Gbit/s error-free wireless on-off-keying data transmission at W-band using an ultra-wideband photonic transmitter-mixer,” *IEEE Photon. J.*, vol. 3, no. 2, pp. 209–219, Apr. 2011.

Jhih-Min Wun was born in Taoyuan, Taiwan, on October 3, 1988. He is currently working toward the Ph.D. degree at the Department of Electrical Engineering, National Central University, Taoyuan. His current research interests include high-speed optoelectronic device measurement and sub-THz high-speed photodiode.

Hao-Yun Liu was born in Hualien City, Taiwan, on November 18, 1991. He received the B.S. degree from the Department of Electrical Engineering, National Tsing-Hua University, Hsinchu City, Taiwan. He is currently working toward the M.S. degree at the Institute of Photonics Technologies, National Tsing-Hua University. His current research interests include high repetition rate pulse laser generation.

Cheng-Hung Lai was born in Miaoli City, Taiwan, on August 12, 1989. He is currently working toward the Master degree at the Department of Electrical Engineering, National Central University, Taoyuan, Taiwan. His current research interests include sub-THz high-speed photodiode.

Yi-Shiun Chen received the Master’s degree from the Institute of Photonics Technologies, National Tsing-Hua University, Hsinchu City, Taiwan. His current research interests include high repetition rate pulse laser generation.

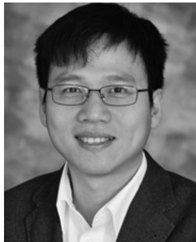

Shang-Da Yang (S'01–M'05) was born in Chiayi, Taiwan, in 1975. He received the B.S. degree in electrical engineering from National Tsing-Hua University, Hsinchu, Taiwan, in 1997, the M.S. degree in electro-optical engineering from National Taiwan University, Taipei, Taiwan, in 1999, and the Ph.D. degree from the School of Electrical and Computer Engineering, Purdue University, West Lafayette, IN, USA, in 2005. He joined National Tsing-Hua University in 2005 as an Assistant Professor and was promoted to Associate Professor in 2010. He received the RiTEK Young Investigator Medal of the Optical Engineering Society of the Republic of China in 2007. He was a Visiting Professor at the Joint Institute for Laboratory Astrophysics, University of Colorado, Boulder, CO, USA, in 2011. His research interests include ultrasensitive femtosecond pulse measurements, characterizations of optical frequency combs, quasi-phase matching engineering, and femtosecond fiber oscillators.

Ci-Ling Pan (M'88–SM'03–F'12) is a Tsing Hua Chair Professor and a Chairperson of the Department of Physics and Institute of Astronomy, National Tsing Hua University (NTHU), Hsinchu, Taiwan. He held joint appointment with the Institute of Photonics Technologies and served as the Director of the Photonics Research Center of NTHU. He was with National Chiao-Tung University, Hsinchu, from 1981 to 2009. He held Visiting Professorship with Osaka University, Osaka, Japan, and Chinese University of Hong Kong, Shatin, Hong Kong, in 2004 and 2008, respectively. His research focuses on ultrafast and THz photonics. His current research interests include the developments of functional liquid crystal THz photonic devices, femtosecond-laser recrystallization and activation of silicon as well as novel THz generators and detectors. The latter have been used in diverse applications, such as diagnostics of technologically important materials for photo-voltaics, assessing burn trauma and optical network- compatible W-band (100 GHz or 0.1 THz) wireless communication link at a data rate beyond 20 Gbit/s. Dr. Pan is a Fellow of APS, OSA, and SPIE.

John E. Bowers (F'93) received the M.S. and the Ph.D. degrees from Stanford University, Stanford, CA, USA. He worked for AT&T Bell Laboratories and Honeywell before joining the University of California, Santa Barbara, CA, USA. He currently holds the Fred Kavli Chair in Nanotechnology, is the Director of the Institute for Energy Efficiency, and is a Professor in the Department of Electrical and Computer Engineering at UCSB. He is a Cofounder of Aurrion, Aerius Photonics, and Calient Networks. He has published eight book chapters, 450 journal papers, 700 conference papers, and has received 52 patents. Dr. Bowers is a Member of the National Academy of Engineering, a Fellow of OSA and the American Physical Society, and a Recipient of the OSA Holonyak Prize, the IEEE LEOS William Streifer Award, and the South Coast Business and Technology Entrepreneur of the Year Award. He and coworkers received the EE Times Annual Creativity in Electronics Award for Most Promising Technology for the hybrid silicon laser in 2007.

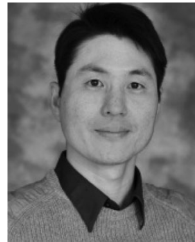

Chen-Bin Huang (M'99–SM'04) received the B.S. degree in electrical engineering from National Tsing Hua University, Hsinchu, Taiwan, in 1997, the M.S. degree in electro-optical engineering from National Chiao Tung University, Hsinchu, in 1999, and the Ph.D. degree from the School of Electrical and Computer Engineering, Purdue University, West Lafayette, IN, USA, in 2008. He has worked at Bell Laboratories (Alcatel-Lucent) in the USA and the Opto-Electronics and Systems Laboratories of the Industrial Technology Research Institute (ITRI) in Taiwan. He has worked as a Visiting Scientist at the Physics Institute, University of Würzburg, Würzburg, Germany, and the Materials Research Institute, Northwestern University, Evanston, IL, USA. He joined the Institute of Photonics Technologies, National Tsing-Hua University, as an Assistant Professor in 2008 and was promoted to Associate Professor in 2012. His current research interests include optical and millimeter-wave arbitrary waveform generations, nanoplasmonics, and applications of optical frequency combs. He has authored/coauthored one book chapter and more than 100 journal and conference papers. He is a holder of seven USA patents and 13 Taiwan patents.

Dr. Huang is a Member of Photonics Society and the Optical Society of America. He has served as a regular Reviewer for *Optics Letters*, *Optics Express*, IEEE JOURNAL OF SELECTED TOPICS IN QUANTUM ELECTRONICS, IEEE PHOTONICS JOURNAL, IEEE PHOTONICS TECHNOLOGY LETTERS, IEEE TRANSACTIONS ON MICROWAVE THEORY AND TECHNIQUES, JOURNAL OF LIGHTWAVE TECHNOLOGY, *Optics Communications*, and *Applied Optics*. He was awarded the Junior Faculty Research Award by the National Tsing Hua University, the Master's Thesis of the Year by the Optical Engineering Society of Republic of China in 1999, Personal Research Achievement Award by OES, and Personal Distinguished Research Achievement Award by ITRI, both in 2002. He received the Andrews and Mary I. Williams Fellowship from Purdue University in 2004 and 2005. He was a Finalist for the IEEE/LEOS 2007 Best Student Paper Award.

Jin-Wei Shi (M'03–SM'12) was born in Kaohsiung, Taiwan, on January 22, 1976. He received the B.S. degree in electrical engineering from National Taiwan University, Taipei, Taiwan, in 1998, and the Ph.D. degree from the Graduate Institute of Electro-Optical Engineering, National Taiwan University, in 2002. He was a Visiting Scholar at the University of California, Santa Barbara (UCSB), CA, USA, from 2000 to 2001. From 2002 to 2003, he served as a Postdoc Researcher at Electronic Research and Service Organization of Industrial Technology Research Institute. In 2003, he joined the Department of Electrical Engineering, National Central University, Taoyuan, Taiwan, where he is currently a Professor. From 2011 to 2013, he joined the ECE Department of UCSB again as a Visiting Scholar. His current research interests include ultra-high speed/power optoelectronic devices, such as photodetectors, electro-absorption modulator, submillimeter wave photonic transmitter, and semiconductor laser. He has authored or coauthored more than four book chapters, 100 Journal papers, 180 conference papers, and holds 30 patents. He was the Invited Speaker of 2002 IEEE LEOS, 2005 SPIE Optics East, 2007 Asia-Pacific Microwave Photonic conference (AP-MWP), 2008 Asia Optical Fiber Communication and Optoelectronic Exposition and Conference, 2012 Optical Fiber Communication (OFC), 2012 Plastic Optical Fiber, and 2012 IEEE Photonic Conference. He served in the Technical Program Committee of OFC 2009–2011, 2012 SSDM, 2012 MWP, 2013 Asia-Pacific CLEO, and 2014 IPRM. He was the Recipient of 2007 Excellence Young Researcher Award from the Association of Chinese IEEE and 2010 Da-You Wu Memorial Award.